Title

Two anterograde intraflagellar transport motors cooperate to build sensory cilia on C-elegans neurons

Journal

Nature Cell Biology, 6(11)

ISSN

1465-7392

Authors

Snow, J J

Ou, G S

Gunnarson, A L

et al.

Publication Date

2004-11-01

Peer reviewed

Two Anterograde Intraflagellar Transport Motors Cooperate to Build Distinct Parts of Sensory Cilia on *Caenorhabditis elegans* Neurons

Joshua J. Snow*, Guangshuo Ou*, Amy L. Gunnarson, Maria Regina Sagullo Walker, H. Mimi Zhou, Ingrid Brust-Mascher and Jonathan M. Scholey.

* These authors contributed equally to this work.

Center for Genetics and Development, Section of Molecular and Cellular Biology, University of California, Davis, CA 95616, USA.

Cilia play diverse roles in motility and sensory reception and their dysfunction contributes to cilia-related diseases. Ciliary assembly and maintenance depends on the intraflagellar transport (IFT) of axoneme, membrane, matrix and signaling proteins to appropriate destinations within the organelle[1-4]. In the current model these diverse cargo-proteins bind multiple sites on macromolecular IFT-particles which are moved by a single anterograde IFT-motor, kinesin II from the ciliary base to its distal tip [5, 6], where cargo-unloading occurs[1-4, 7]. Here we watched fluorescent IFT-motors and IFT-particles moving along distinct domains within sensory cilia of wild-type and IFT-motor-mutant *C. elegans*, and show that two anterograde IFT-motor holoenzymes, kinesin-II and Osm-3-kinesin [8] cooperate in a surprising way to drive two pathways of IFT that build distinct parts of cilia. Instead of each motor independently moving its own specific cargo to a distinct destination, the two motors function redundantly to transport IFT-particles along doublet microtubules (MTs) adjacent to the transition zone to form the axoneme middle segment [9] and then Osm-3-kinesin alone transports IFT-particles along the distal singlet MTs to stabilize the distal segment.

Following the loss of heterotrimeric kinesin-II function, some membrane proteins are delivered normally to ciliary membranes[10] and distinct parts of axonemes can still assemble [11]. Therefore, in contrast to the accepted single pathway mechanism of IFT [1-4], it is possible that multiple pathways deliver ciliary cargo molecules to distinct sites to build discrete parts of cilia, reminiscent of the multiple transport pathways operating in axons [7, 12, 13].

Sensory [9] and motile [14] axonemes are differentiated longitudinally into two domains, the "middle segment" and "distal segment" consisting of 9 doublet and 9 singlet MTs, respectively (Figure 1). To investigate if these two domains could be built by distinct IFT pathways we watched the motility of specifically-labeled IFT-motors and IFT-particles within sensory cilia on chemosensory neurons of *C. elegans* using time-lapse fluorescence microscopy [15]. Previously we observed IFT-particles moving base-to-tip at unitary rates of 0.7μm/s [15, 16], but with improved optics and kymography [17] we find that IFT-particles move anterogradely at two rates; 0.7μm/s along the middle segment then accelerating to 1.3 μm/s along the distal segment (Figs. 2, S1; Table 1). No significant difference in retrograde transport along the two segments was observed (V_{middle} = 1.17 +/- 0.25 μm/s, n = 49; V_{distal} = 1.09 +/- 0.25 μm/s, n = 43).

Biochemical fractionation and localization suggested that these cilia contain two candidate anterograde IFT motors, heterotrimeric kinesin-II (consisting of 1 KRP85 motor : 1 KRP95motor : 1 accessory KAP encoded by *klp-11, klp-20* and *kap-1*) and

homodimeric Osm-3-kinesin (2 x OSM-3) [8]; cilia in *osm-3* mutants lack their distal segments[9] suggesting a role in ciliogenesis but the function of kinesin-II in this system is unknown. We watched these motors moving along middle and distal segments *in vivo*, and find that Osm-3-kinesin moves the full length of the axoneme at the same two rates as IFT-particles, but kinesin-II only moves along the middle segment and never enters the distal segment (Table 1; Figure S2).

To understand the significance of these differences, we sought loss-of-function mutants defective in kinesin-II and Osm-3-kinesin function. Seven *osm-3* mutant alleles have long existed, and mutants in KRP95 and KAP subunits [8] were recently obtained by the *C. elegans* gene knock-out consortium [18]. We sequenced the DNA of all these mutants to deduce their molecular lesions, and used standard "dye-filling" and osmotic avoidance assays to assess ciliary structure and function [9, 19] (Table 2). Despite two "nonconformists" (*osm-3* alleles *mn391* and *n1540/n1545*) these assays are useful indicators of ciliary performance (although we show later that direct assays of IFT can be more illuminating).

As shown before, mutants containing the severe *osm-3(p802)* allele that lack ciliary distal segments display defective dye-filling and osmotic avoidance [9, 19] and our sequencing indicates this allele may encode a motor subunit that lacks the stalk-tail domains and is unlikely to bind IFT-particles. In contrast, animals carrying single KRP95 and KAP mutants display no dye-filling or osmotic avoidance defects. The lesion in the KRP95 mutant *klp-11 (tm324)* only truncates the tail domain which would predict a weak

phenotype (but note that a similar *osm-3* mutant, (*e1811*) displays defective dye-filling and osmotic avoidance). The *kap-1(ok676)* mutant, however, is severely truncated lacking all its protein-interacting armadillo repeats, suggesting it is likely to be a severe loss-of-function allele, yet unlike *Drosophila* KAP mutants [20], it apparently has normal cilia and thus displays no defects in dye-filling or osmotic avoidance (but see later).

Kinesin-II is multifunctional, driving critical organelle, protein and RNA transport events outside cilia[21-23] so it is possible that kinesin-II performs non-ciliary functions in *C. elegans* with Osm-3-kinesin substituting as an IFT motor. Alternatively redundancy may be involved; some single kinesin-II subunit knock-outs yield no phenotype [24, 25] apparently in one case because of functional redundancy between the two motor subunits of this heterotrimeric complex [25]. In *C. elegans*, could the kinesin-II and Osm-3-kinesin holoenzymes [8] have redundant ciliary functions?

To test this, we crossed *osm-3(p802)* and *kap-1(ok676)* worms to produce double mutants with impaired kinesin-II and Osm-3-kinesin function and looked at the distribution of the IFT-particle subunit, OSM-6::GFP, along the cilia of single and double mutant animals (Fig. 1). In KAP single mutants, IFT particle fluorescence extends the same distance (7-8μm) from the transition zone (TZ) as in wild type animals, suggesting that in the absence of KAP function, IFT particles are transported normally all along the axoneme. In *osm-3* mutants lacking distal segments [9], IFT-particle fluorescence extends only 4-5μm from the TZ, consistent with the hypothesis that in the absence of Osm-3-kinesin function, kinesin-II drives IFT-particle transport along the middle segment remnants. In

kap-1: osm-3 double mutants however, IFT-particle fluorescence does not extend along the cilia at all, but instead accumulates at the TZ (Fig. 1), indicating that in the absence of both motors, IFT ceases and IFT-particles are not moved away from the TZ [9]. Thus we hypothesize that kinesin-II and Osm-3-kinesin play redundant roles in driving IFT along the middle segments of the cilia, whereas Osm-3-kinesin, but not kinesin-II, drives IFT along the distal segment.

Results from IFT motility assays were consistent with this idea (Table 1; Fig. S1). In an Osm-3-kinesin mutant background, IFT-particles moved only along the middle segments at the characteristic slow rate and we observed no transport along the distal segments. As expected, in the *kap-1; osm-3* double mutants, no IFT-particle motility was observed. However, it was striking that in *kap-1* single mutants, IFT particles moved the full length of the axoneme as in wild-types, consistent with the OSM-6::GFP distribution, but at a constant base-to-tip rate of 1.3 μm/s, similar to the faster distal-segment transport in wild-types.

The subtle phenotype displayed by the *kap-1* single mutant, i.e. accelerated IFT along the middle segment, suggests, surprisingly, that in wild-type animals both Osm-3-kinesin and kinesin-II move the same IFT-particles along the middle-segment, with the slower moving kinesin-II (0.5μm/s) exerting drag on the faster moving Osm-3-kinesin (1.3 μm/s), giving rise to the intermediate rate of transport observed (0.7μm/s). We propose that at the middle segment tip IFT-particles reorganize, allowing kinesin-II to unload its cargo and undergo turnaround while Osm-3-kinesin-bound particles are liberated to move

unrestrained to the distal segment tip at the faster rate characteristic of Osm-3-kinesin. This generates two sequential IFT pathways (Fig. 2B). In the "middle segment" pathway, kinesin-II and Osm-3-kinesin act redundantly to transport IFT-particles and either motor, but not both, is dispensable for this, then in the "distal segment" pathway, Osm-3-kinesin acts alone to transport IFT-particles to the distal tip.

What is the functional significance of having two IFT pathways? It is likely that these pathways build distinct parts of the ciliary axoneme. Thus, in the absence of kinesin-II, Osm-3-kinesin can assemble, and move along, a full-length axoneme; in the absence of Osm-3-kinesin the distal segment is missing, but an apparently normal middle segment remains, plausibly built by kinesin-II which drives IFT along it; in the absence of both kinesin-II and Osm-3-kinesin, IFT is abolished, IFT-particles accumulate at the TZ and no axoneme is built, in accordance with the phenotype of IFT-particle mutants [9]. Thus kinesin-II and Osm-3-kinesin act redundantly to build the middle segment, whereas Osm-3-kinesin is essential for distal segment assembly. This could be accomplished if, for example, the cargo of kinesin-II and Osm-3-kinesin (K and O in fig. 2B) are axoneme-stabilizing factors, eg MAPs, with either cargo being capable of stabilizing the middle segment, but the Osm-3-cargo being uniquely required for distal segment stabilization. Another possibility is that one or both motors could deliver distinct signaling molecules that control axoneme length, similar to the "long flagella" (LF4) MAP kinase or the *Chlamydomonas* aurora-like kinase (CALK) [26, 27].

This is the first demonstration that two distinct anterograde IFT-motor holoenzymes participate in IFT, raising the question of its generality. The cilia of *Tetrahymena* contain homologs of KRP85, KRP95 and OSM-3 [25, 28], but unlike in *C. elegans* their oligomerization state and ability to move along cilia are unexplored. In sea urchin embryos [11] and *Chlamydomonas* [6], kinesin-II appears to be the dominant IFT-motor, but Osm-3-kinesin could assemble the procilium that initiates ciliogenesis[11] and drive the transient elongation of the distal segments of the axoneme during mating[14].

Thus *C. elegans* sensory cilia use two sequential IFT pathways, a "middle-segment" pathway dependent on kinesin-II and Osm-3-kinesin, and a "distal segment" pathway dependent on Osm-3-kinesin alone. The subtle manner in which the two motors are deployed, having distinct yet partially overlapping functions, is striking. Functional cooperation and redundancy between mitotic motor holoenzymes is common, but to our knowledge this is the first such example pertaining to kinesins involved in intracellular transport. Moreover this indicates that IFT may be more complex and fascinating than we appreciate; given the large range of cargo that must be delivered to cilia, perhaps two IFT pathways operating in a single cilium is the "tip of the iceberg", and additional pathways may contribute to the delivery of ciliary components.

Methods:

Fluorescence Microscopy: Intraflagellar transport was assayed as described previously [15-17]. Images were collected on an Olympus microscope equipped with a 100X, 1.35 NA objective and an Ultraview spinning disc confocal head[17] at 2-3 frames/second for 2-3

mins, with the transgenic worms anesthetized with 10mM levamisole, mounted on agarose pads and maintained at 21ºC. Kymographs and movies were created using Metamorph software. The length distribution of OSM-6::GFP along sensory cilia was determined by densitometry of confocal images of live transgenic animals.

Creation and Maintenance of Transgenic and Mutant Animals: We periodically requested kinesin-II mutants from the *C.elegans* gene knock-out consortium, who produced mutants in the KRP95 *(klp-11(tm324))* and KAP (*kap-1(ok676)*) subunits by UV-trimethyl-psoralen mutagenesis [18] and kindly provided us with them. They were outcrossed multiple times and these, the *osm-3* mutant strains, and the GFP-IFT-protein expressing strains were maintained using standard procedures [16, 17].

Characterization of Mutants: Genomic sequences were obtained by PCR amplification from single worms or genomic extracts. cDNAs were prepared by RT-PCR on total RNA extracts. For each allele, molecular lesions were confirmed by multiple sequence alignment from 3-4 independent PCR reactions using Pileup and Pretty sequence analysis software. Dye-filling and osmotic avoidance assays were performed as described [9, 19].

Genetic Crosses: To create double motor mutants expressing IFT-particle::GFP transgenes, males expressing OSM-6::GFP were crossed with homozygous mutant *kap-1* hermaphrodites, and the F1 heterozygotes were selfed to obtain *kap-1(ok676)III; mnIs17*[*osm-6::GFP*] progeny. *Osm-3(p802)IV; mnIs17[osm-6::GFP]* males were crossed with homozygous *kap*-1 hermaphrodites, and the F1 heterozygotes were selfed to *kap-1(ok676)III; osm-3(p802)IV; mnIs17 [osm-6::GFP]* progeny. Homozygosity was confirmed for *osm-3(p802)IV* by dye filling and for *kap-1(ok676)III* by single-worm PCR.

References:

1. Rosenbaum, J.L. and Witman, G.B. (2002) Intraflagellar Transport. Nature Reviews Molecular Cell Biol., **3**, 813-825.

2. Scholey, J.M. (2003) Intraflagellar Transport. Ann. Rev. Cell Dev. Biol., **19**, 423-443.

3. Snell, WJ, Pan, J, Wang, Q (2004) Cilia and Flagella Revealed: From Flagellar Assembly in *Chlamydomonas* to Human Obesity Disorders. Cell, **117**, 693-697.

4. Pazour, GJ and Witman, GB (2003) The vertebrate primary cilium is a sensory organelle. Curr. Op. Cell Biol., **15**, 105-110.

5. Cole, DG, Chinn SW, Wedaman, KP, Hall K, Vuong, T, Scholey, JM (1993) Novel Heterotrimeric Kinesin-related Protein Purified from Sea Urchin Eggs. Nature, **366**, 268-270.

6. Cole, DG, Diener, DR, Himelblau, AL, Beech, PL, Fuster, JC and Rosenbaum, JL (1998) *Chlamydomonas* kinesin-II-dependent intraflagellar transport (IFT): IFT particles contain proteins required for ciliary assembly in *Caenorhabditis elegans* sensory neurons. J. Cell Biol., **141**, 993-1008.

7. Vale, R.D. (2003) The Molecular Motor Toolbox for Intracellular Transport. Cell. **112**, 467-480.

8. Signor, D, Wedaman, KP, Rose, LS, Scholey, JM (1999) Two Heteromeric Kinesin Complexes in Chemosensory Neurons and Sensory Cilia of *Caenorhabditis elegans.* Mol. Biol. Cell, **10**, 345-360.

9. Perkins, LA, Hedgecock, EM, Thomson, JN, Culotti, JG (1986) Mutant Senssory Cilia in the Nematode *Caenorhabditis elegans.* Dev. Biol., **117**, 456-487.

10. Pan J, and Snell WJ (2002) Kinesin-II is required for flagellar sensory transduction during fertilization in *Chlamydomonas*. Mol. Biol. Cell, **13**, 1417-1426.

11. Morris, RL and Scholey, JM (1997) Heterotrimeric kinesin-II is required for the assembly of Motile "9+2" ciliary axonemes on Sea Urchin Embryos. J. Cell Biol., **138**, 1009-1022.

12. Miki, H, Setou, M, Kaneshiro, K, Hirokawa, N (2001) All kinesin superfamily protein, KIF, genes in mouse and human. PNAS. **98**, 7004-7011.

13. Goldstein, LSB and Yang, Z (2000) Microtubule-based transport systems in neurons. The roles of kinesins and dyneins. Ann. Rev. Cell. Dev. Biol., **23,** 39-71.

14. Mesland, DAM, Hoffman, JL, Caligor, E, Goodenough, UW (1980) Flagellar Tip Activation Stimulated by Membrane Adhesions in *Chlamydomonas* Gametes. J. Cell Biol., **84**, 599-617.

15. Orozco, JT, Wedaman, KP, Signor, D, Brown, H., Rose, L, Scholey, JM (1999) Movement of Motor and Cargo Along Cilia. Nature, **398**, 674.

16. Signor, D, Wedaman, KP, Orozco, JT, Dwyer, ND, Bargmann, CI, Rose LS, Scholey JM (1999) Role of a Class DHC1b Dynein in Retrograde Transport of IFT Motors and IFT Raft Particles Along Cilia, but not Dendrites, in Chemosensory Neurons of Living *Caenorhabdidtis elegans.* J. Cell Biol., **147**, 519-530.

17. Zhou HM, Brust-Mascher I, and Scholey JM (2001) Direct visualization of the Movement of the Monomeric Axonal Transport Motor, UNC-104 along neuronal Processes in Living *C. elegans.* J. Neurosci., **21,** 3749-3755.

18. Yandell MD, Edgar LG and Wood WB (1994) Trimethylpsoralen induces small deletion mutations in Caenorhabditis elegans. Proc Natl Acad Sci U S A, **91**,1381-5.

19. Starich, TA, Herman, RK, Kari, WH, Yeh, WS, Schackwitz, M., Schuyler, J, Collet, J, Thomas, J, Riddle, D (1995) Mutations affecting chemosensory neurons of *Caenorhabditis elegans.* Genetics, **139**, 171-188.

20. Sarpal R., Todi SV, Sivan-Loukianova E, Shirolikar S, Subramanian N, Raff EC, Erickson JW, Ray K, Ebert DF (2003) *Drosophila* KAP interacts with the Kinesin II Motor subunit KLP64D to assemble Chordotonal Sensory Cilia but not Sperm Tails. Current Biol., **13**, 1687-1696.

21. Fan, J and Beck, KA (2004) A role for the spectrin superfamily member Syne-1 and kinesin II in cytokinesis. J. Cell Sci., **117**, 619-629.

22 Bentley, JN, Heinrich, B, Vernos, I, Sardet, C., Prodon, F., Deshler, JO (2004) Kinesin II mediates Vg1 mRNA transport in *Xenopus* Oocytes. Current Biol., **14**, 219-224.

23. Kawasaki, Y, Koyama, A, Sato, R, Takada, S, Haraguchi, K, Akiyama, T (2002) Identification of a link between the tumour suppressor APC and the kinesin superfamily. Nat Cell Biol. **4,** 323-327.

24. Yang Z, Roberts EA, Goldstein LSB (2001) Functional analysis of Mouse Kinesin Motor Kif3C Mol. Cell Biol. **21**, 5306-5311.

25. Brown, JM, Marsala, C, Kosoy, R, Gaertig J (1999) Kinesin II is preferentially targeted to assembling cilia and is required for ciliogenesis and normal cytokinesis in *Tetrahymena*. Mol Biol. Cell., **10**, 3081-3091.

26. Berman SA, Wilson NF, Haas NA, Lefebvre P (2003) A novel MAP kinase regulates flagellar length in *Chlamydomonas*. Curr. Biol., **13**, 1145-1149.

27. Pan J, Wang Q and Snell WJ (2004) An aurora kinase is essential for flagellar disassembly in *Chlamydomonas*. Dev. Cell, **6**, 445-451.

28. Awan A., Bernstein, M, Hamasaki, T, Satir, P (2004) Cloning and characterization of Kin5, a Novel *Tetrahymena* Ciliary Kinesin II. Cell Motility and the Cytoskeleton. **58**, 1-9.

29. Bargmann, C. and Mori, I. (1997) Chemotaxis and Thermotaxis in *C. elegans* II (Riddle, D, Blumenthal, T, Meyer, BJ, Priess, JR eds) pp 717-737, Cold Spring Harbor Laboratory Press, Cold Spring Harbor, NY.

30. Pierce-Shimomura, JT, Morse, TM, Lockery, SR (1999) The fundamental Role of Pirouettes in *Caenorhabdidtis elegans* chemotaxis. J. Neurosci., **19**, 9557-9569.

Acknowledgements: We thank Dr G. Civelekoglu-Scholey for Figure 2B, and, Drs L. Rose, F. McNally, KB Kaplan, D Starr, W. Snell, J. Pan and many members of the IFT and *C. elegans* communities for encouragement and discussion. We thank Theresa Stiernagle, Robert Herman and the *C. elegans* gene knockout consortium for providing kinesin-II mutants. Supported by a grant from the National Institutes of Health.

Table 1. Velocity of IFT-motors and IFT-particles along middle and distal segments of ciliary axonemes in wild-type, *osm-3* and *kap-1* mutant animals.

Transgenic strain		Average velocities (μm s^{-1})			
		Middle segment (N)		Distal segment (N)	
IFT particles	OSM-6::GFP	0.68 ± 0.10	(339)	1.27 ± 0.19	(303)
IFT motors	OSM-3::GFP	0.72 ± 0.14	(265)	1.28 ± 0.15	(277)
	KAP-1::GFP	0.65 ± 0.10	(245)	None	
IFT particles (OSM-6::GFP) in motor mutants	*osm-3(p802)*	0.52 ± 0.07	(260)	None	
	kap-1(ok676)	1.20 ± 0.17	(254)	1.27 ± 0.16	(253)
	kap-1 (ok676);osm-3 (p802)	None		None	

(N) = Number of GFP particles.

Table 2. Characterization of kinesin-II and Osm-3-kinesin mutant Alleles.

	Allele	Residues	Mutation	Dye filling	Osmotic avoidance
A.	WT OSM-3	1-699		+	+
	p802	1-345	Q346-stop	-	-
	mn391	1-438	Q349-stop	-	+
	sa125	1-699	G444E	-	-
	n1540/n1545	1-699	Q98P,D150N	+	-
	e1811	1-578	W579-stop	-	-
	mn357	1-265	frameshift termination	-	-
	sa131		not expressed	-	-
B.	WT KRP95	1-782		+	+
	tm324	1-607	T608-stop	+	+
	WT KRP85	1-646		+	+
	WT KAP-1	1-679		+	+
	ok676	1-121	frameshift termination	+	+

Protein sequences of Osm-3-kinesin (A) and kinesin-II (B) mutants were deduced from genomic and cDNA sequencing. Wild-type OSM-3 motor = 1-323, neck = 324-359, rod = 360-523, tail = 524-699; KRP95 motor = 1-340, neck = 341-382, rod = 383-566, tail 567-782; KRP85 motor = 1-340, neck = 341-382, rod = 383-566, tail 567-645. Wild-type

KAP has armadillo repeats at residues 215-253, 255-297, 299-338, 340-379, 416-456, 552-593 and 596-636. A 4 b.p. insert truncates allele mn357. No cDNA could be amplified for *sa131* suggesting no expression. The KAP-1 ok676 allele contains a 989 b.p. deletion and a 3 b.p. insertion so the cDNA splices out of frame and encodes 113 wild-type residues, 8 missense residues and a stop. Animals were assayed for dye-filling and osmotic avoidance [9, 19].

Figure Legends:

Figure 1. **Sensory cilia on neurons of wild-type and mutant C. elegans.** A. Chemotaxis depends on the detection of environmental chemicals by chemoreceptors concentrated in the membranes surrounding the nonmotile axonemes of sensory cilia on chemosensory neurons [9, 19, 29, 30]. Their axonemes are 7.5 µm long, consisting of a 1 µm long basal body, the transition zone (TZ), a 4 µm long "middle segment" consisting of nine doublet MTs, and a 2.5 µm "distal segment" consisting of nine singlet MTs that extend from the middle segment A subfibers. GFP::IFT proteins (green) accumulate in the TZ and move anterogradely along the middle and distal segments to the tip (arrows). B. Fluorescence micrographs and corresponding cartoons of the distribution of IFT-particles (OSM-6::GFP) along sensory cilia (asterisk = TZ; arrowhead = middle segment; arrow = distal segment) in (a) wild-type (b) *kap-1* mutant, (c) *osm-3*-mutant (missing distal segment) and (d) *kap-1; osm-3* double mutant (missing middle and distal segments) animals. Numbers = length, with n = # animals, m = # cilia measured. Bar = 3 µm.

Figure 2: Anterograde IFT along middle and distal segments of sensory cilia. A. Motility of OSM-6::GFP within sensory cilia of wild-type animals. Left panel, fluorescence micrographs with corresponding cartoon showing the lines used to generate kymographs along 4 middle segments (M1-M4) and the distal segment (D). Kymographs (M1-M4 and D) and corresponding lines (M1'-M4' and D') show that motility along distal segment is faster than along middle segments. Horizontal bars = 2.5 μm. Vertical bar = 5s. B. Model showing sequential "middle" (large arrows) and "distal" (small arrows) IFT-pathways. Following assembly of IFT machinery and its entry into cilium (step 1), IFT-particles are moved anterogradely by kinesin-II and Osm-3-kinesin at 0.7μm/s along the middle segment with kinesin-II exerting drag (step 2). Kinesin-II undergoes turnaround (step 3), and liberated Osm-3-kinesin-bound IFT particles move at 1.3 μm/s to the distal tip (4) where Osm-3-kinesin turnaround occurs. Recycling involves retrograde transport (steps 6,7) and disassembly (8). In this model the cargo of kinesin-II (K) and Osm-3-kinesin (O) are axoneme-stabilizing factors. Either factor can stabilize middle segment doublets, but O is essential to stabilize distal singlets.

Figure S1: Anterograde transport of IFT-particle along middle and distal segments of sensory cilia. Motility of IFT particle (OSM-6::GFP) within sensory cilia of wild-type (A),osm-3 mutant (B) and kap-1 mutant (C). Left column show fluorescence micrographs with corresponding cartoon showing the lines used to generate kymographs along 4 middle segments (M1-M4) and the distal segment (D). Kymographs (middle column) show that motility along distal segment is faster than along middle segments (no distal segment motility is seen in osm-3). Right column, histograms showing IFT

velocity profiles along middle and distal segments (see Table 1 and text). Horizontal bars = 2.5 μm. Vertical bar = 5s.

Figure S2: Anterograde transport of IFT-motors along middle and distal segments of sensory cilia. Motility of IFT motors within sensory cilia of wild-type, OSM-3::GFP (A) and KAP-1::GFP (B). Left column show fluorescence micrographs with corresponding cartoon showing the lines used to generate kymographs along 3 middle segments (M1-M3) and the distal segment (D). Kymographs (middle column) show that motility of OSM-3::GFP along distal segment is faster than along middle segments whereas KAP::GFP never enters distal segment and only moves in middle segment at a slow velocity. Right column, histograms showing IFT velocity profiles along middle and distal segments (see Table 1 and text). Horizontal bars = 2.5 μm. Vertical bar = 5s.

Movies 1-3 Transport of IFT-particle (OSM-6::GFP) along sensory cilia. Wild-type (Movie 1), *osm-3*(p802) mutant (Movie 2) and *kap-1*(ok676) mutant (Movie 3).

Movie 4-5 Transport of IFT motors OSM-3-kinesin (OSM-3::GFP, Movie 4) and Kinesin-II (KAP-1::GFP, Movie 5) along sensory cilia.
The display rate of the movies is 10 frames per second with total elapsed time of 90s.

Correspondence and materials requests should be directed to Jonathan M. Scholey (jmscholey@ucdavis.edu).

Figure 1

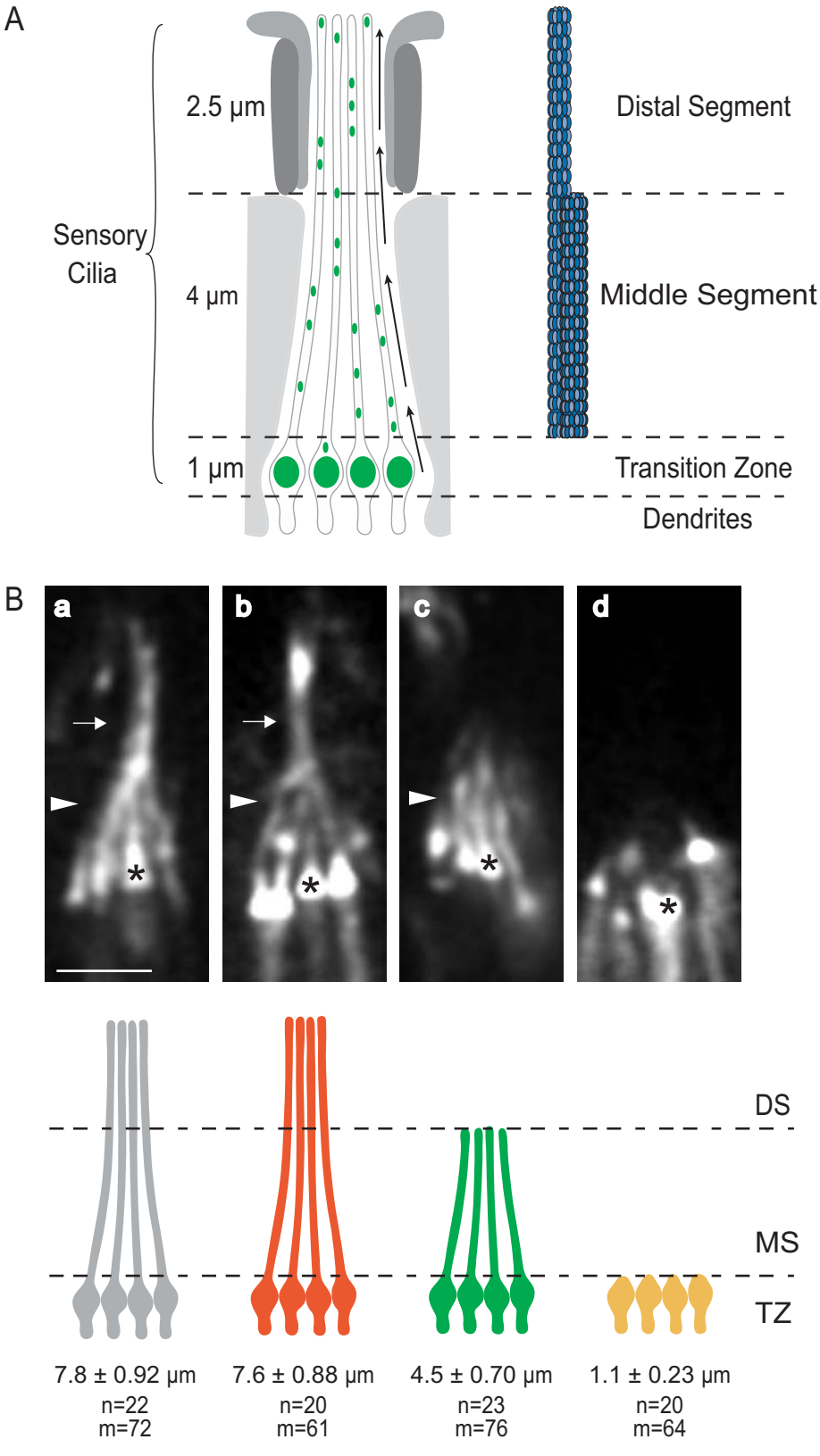
A
2.5 µm
Distal Segment
Sensory
Cilia
4 µm
Middle Segment
1 µm
Transition Zone
Dendrites
B
a
b
c
d
DS
MS
TZ
7.8 ± 0.92 µm
n=22
m=72
7.6 ± 0.88 µm
n=20
m=61
4.5 ± 0.70 µm
n=23
m=76
1.1 ± 0.23 µm
n=20
m=64

Figure 2

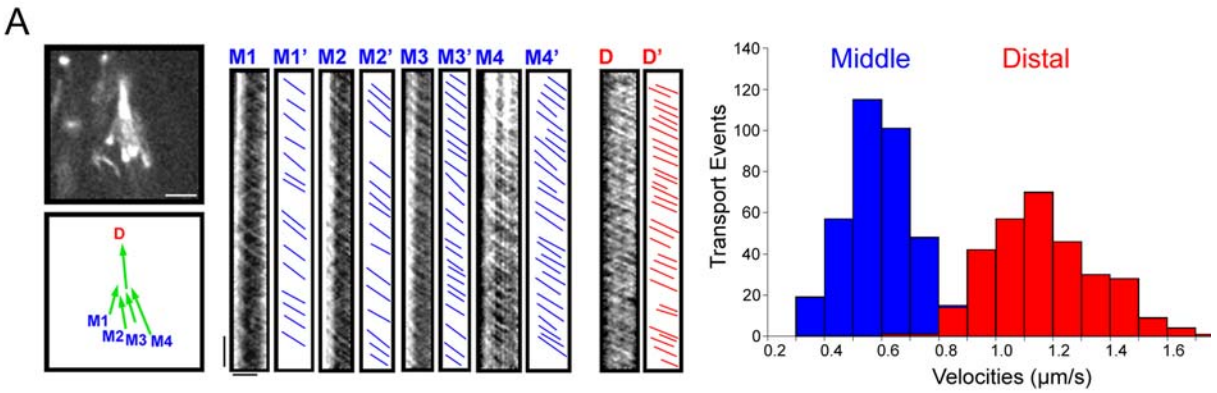
A
M1
M1'
M2
M2'
M3
M3'
M4
M4'
D
D'
Middle
Distal
Transport Events
Velocities (μm/s)

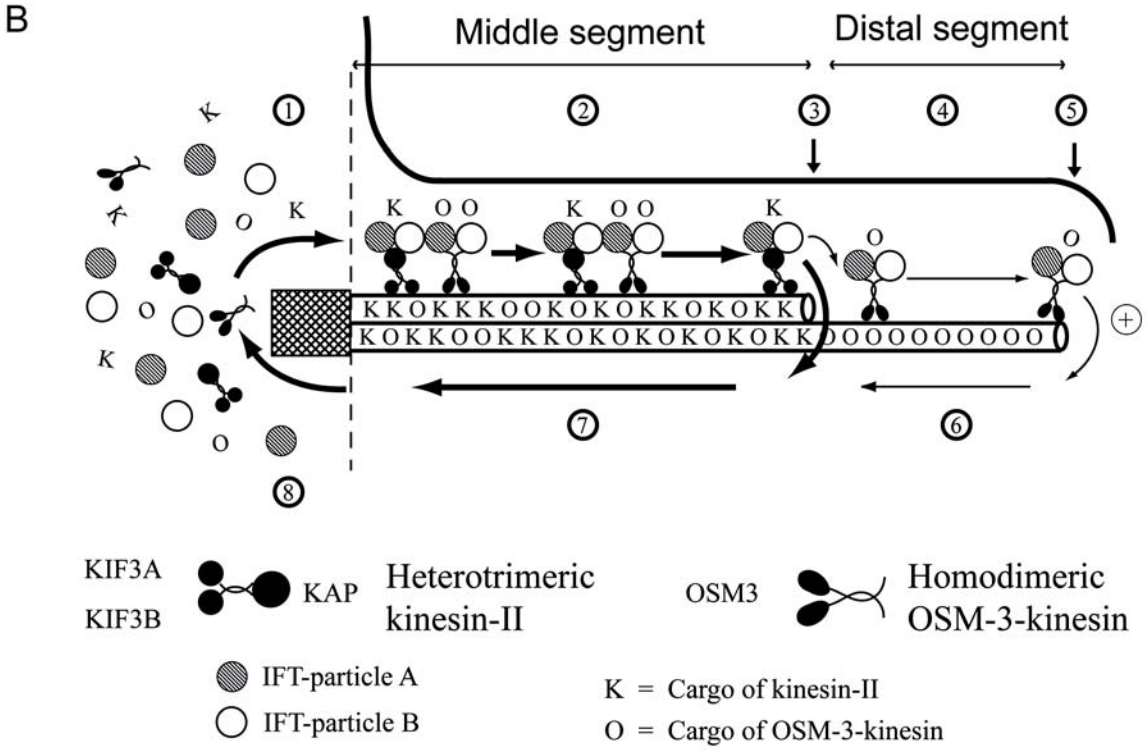
B
Middle segment
Distal segment
KIF3A
KIF3B
KAP
Heterotrimeric kinesin-II
OSM3
Homodimeric OSM-3-kinesin
IFT-particle A
IFT-particle B
K = Cargo of kinesin-II
O = Cargo of OSM-3-kinesin

Figure S1

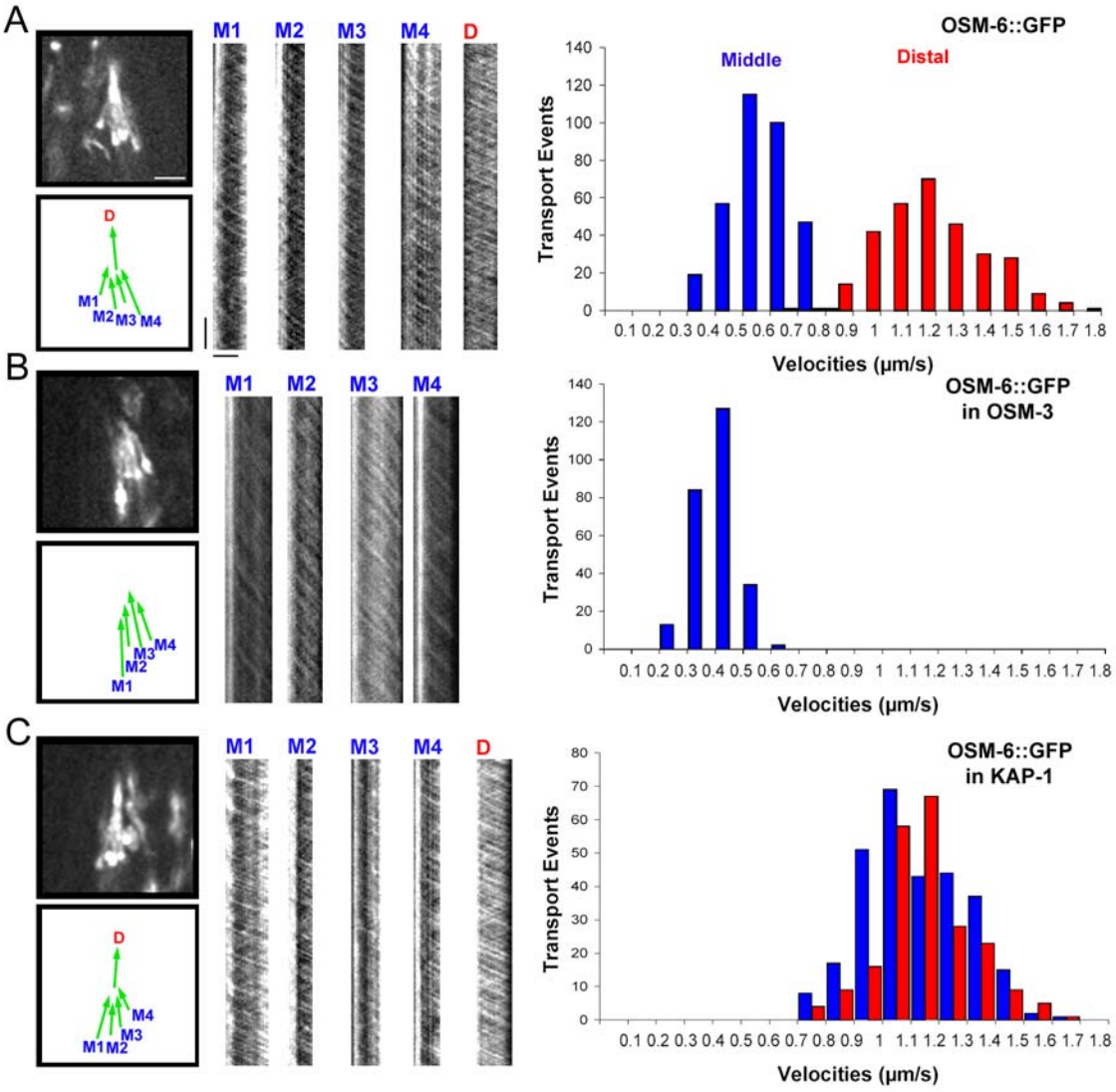
A
M1
M2
M3
M4
D
OSM-6::GFP
Middle
Distal
Transport Events
Velocities (µm/s)
B
OSM-6::GFP
in OSM-3
C
OSM-6::GFP
in KAP-1

Figure S2

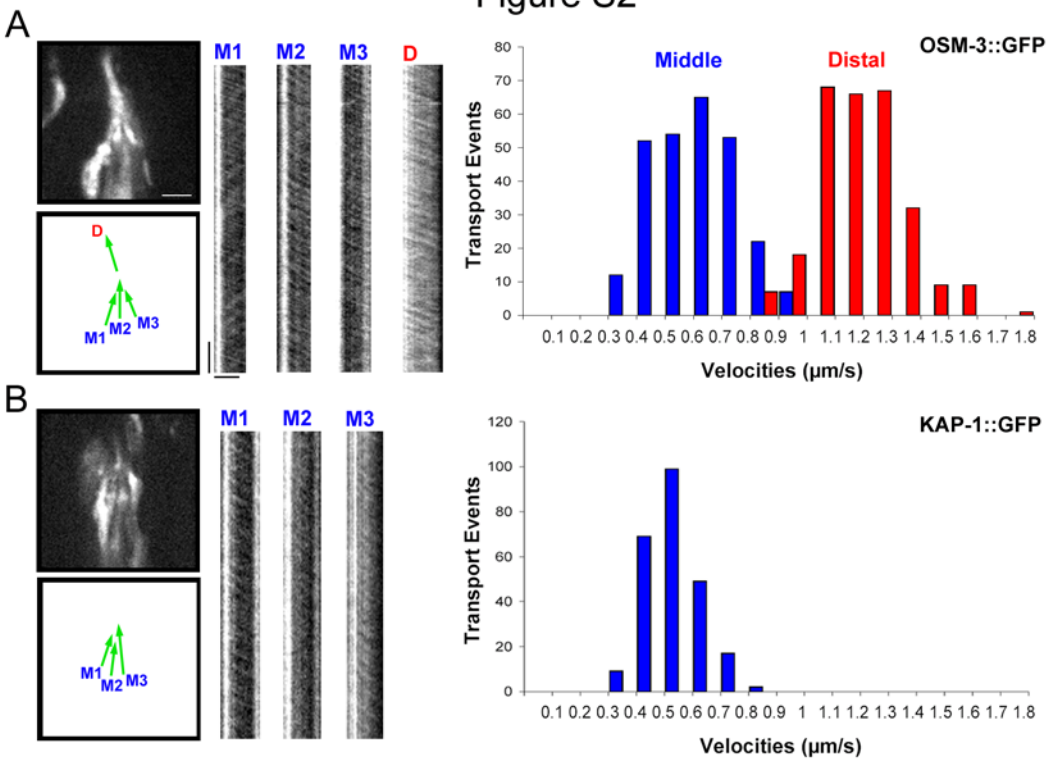
A
M1
M2
M3
D
D
M1
M2
M3
OSM-3::GFP
Middle
Distal
Transport Events
Velocities (μm/s)
B
M1
M2
M3
M1
M2
M3
KAP-1::GFP
Transport Events
Velocities (μm/s)